

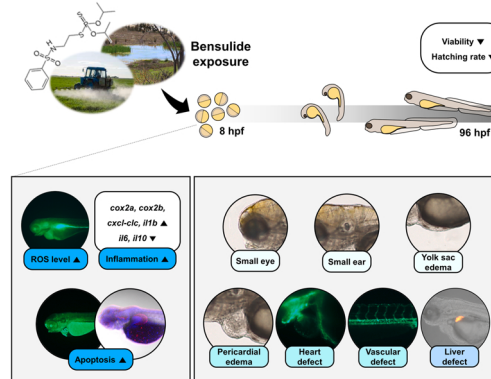
## Research Article

Bensulide-induced oxidative stress causes developmental defects of cardiovascular system and liver in zebrafish (*Danio rerio*)Miji Kim <sup>a,1</sup>, Garam An <sup>a,1</sup>, Junho Park <sup>a</sup>, Gwonhwa Song <sup>a,\*</sup>, Whasun Lim <sup>b,\*</sup><sup>a</sup> Institute of Animal Molecular Biotechnology and Department of Biotechnology, College of Life Sciences and Biotechnology, Korea University, Seoul 02841, Republic of Korea<sup>b</sup> Department of Biological Sciences, Sungkyunkwan University, Suwon 16419, Republic of Korea

## HIGHLIGHTS

- Bensulide induces developmental malformations in zebrafish larvae.
- Bensulide triggers apoptosis, cell cycle arrest, and ROS production in zebrafish.
- Bensulide causes defects in heart and liver development during embryogenesis.
- Bensulide may cause pollution and has detrimental effects on aquatic environments.

## GRAPHICAL ABSTRACT



## ARTICLE INFO

Editor: Lingxin CHEN

## Keywords:

Organophosphate herbicide  
Reactive oxygen species  
Aquatic organisms  
Heart development  
Hepatogenesis

## ABSTRACT

Bensulide is an organophosphate herbicide commonly used in agricultural crops; however, no studies have reported on its toxic effects in the embryonic development of vertebrates, particularly gene expression level and cellular response. Therefore, to identify developmental toxicity, zebrafish eggs 8 h post-fertilization (hpf) were exposed to bensulide concentrations of up to 3 mg/L. The results indicated that exposure to 3 mg/L bensulide inhibited the hatching of all eggs and decreased the size of the body, eyes, and inner ear. There were demonstrated effects observed in the cardiovascular system and liver caused by bensulide in *fli1:eGFP* and *L-fabp:dsRed* transgenic zebrafish models, respectively. Following exposure to 3 mg/L bensulide, normal heart development, including cardiac looping, was disrupted and the heart rate of 96 hpf zebrafish larvae decreased to 16.37%. Development of the liver, the main detoxification organ, was also inhibited by bensulide, and after exposure to 3 mg/L bensulide its size reduced to 41.98%. Additionally, exposure to bensulide resulted in inhibition of antioxidant enzyme expression and an increase in ROS levels by up to 238.29%. Collectively, we identified various biological responses associated with the toxicity of bensulide, which led to various organ malformations and cytotoxic effects in zebrafish.

\* Corresponding authors.

E-mail addresses: [ghsong@korea.ac.kr](mailto:ghsong@korea.ac.kr) (G. Song), [wlim@skku.edu](mailto:wlim@skku.edu) (W. Lim).<sup>1</sup> These authors contributed equally to this work.

## 1. Introduction

Owing to a wide range of benefits, pesticides are widely used in industrialized agriculture [1]. However, pesticides pose risks to non-target organisms and the environment. Therefore, research on the effects of hazardous pesticides is important [2]. Bensulide, a pre-emergence organophosphate herbicide, acts as a lipid synthesis and cell division inhibitor and is used on crops, such as vegetables, legumes, and garlic [3]. The U.S. Geographical Survey's Pesticide National Synthesis Project reported that approximately 0.5–0.7 million pounds of bensulide are used annually [4].

Owing to its widespread usage, numerous studies have investigated the environmental distribution and persistence of bensulide. Bensulide has been reported to persist in the soil for 8–34 days, 91–210 days, and over a year in California, Mississippi, and Texas, respectively [5]. The high organic carbon absorption coefficient ( $K_{OC} = 3900 \text{ mL/g}$ ) of bensulide suggests that it can be adsorbed onto organic compounds in the soil and remain near the surface [6]. This allows such pesticides to be transported to rivers through surface runoff caused by rainfall, and thus possibly contaminating aquatic environments [3]. The mean runoff concentration of bensulide from golf course greens in Boston, Philadelphia, and Rochester was 0.082–0.175 mg/L [6]. Additionally, the presence of bensulide in some human urine samples suggests that this pesticide poses high risks for human exposure and persistence in the body [7].

Given its long half-life, potential for bioaccumulation, and outflow to other regions, it is crucial to elucidate the hazards of bensulide on non-target organisms to preserve ecosystems and human health. Several studies have investigated the adverse impacts of this herbicide. At a concentration of approximately 40 mg/L, bensulide was observed to almost completely inhibit the *in vitro* growth of leukemia and lymphoma cells in mice [8]. In another study, one-year-old channel catfish (*Ictalurus punctatus*) showed 10% mortality after exposure to 10 mg/L bensulide for 48 h [9]. Furthermore, reproductive and developmental toxicities have been identified. Exposure of bensulide at 80 mg/kg/day inhibited normal vascular development, causing miscarriages in rabbits [10]; and at concentrations of 1000 mg/L it adversely affected the hatchability of Japanese quail [11]. However, few studies have comprehensively reported the biological responses to bensulide exposure during embryonic development. Analyzing the biological responses to bensulide is essential to elucidating its developmental toxicity and provides information for demonstrating its toxic mechanisms. Thus, zebrafish were utilized to investigate the developmental toxicity of bensulide.

To study the adverse effects of pesticides on vertebrate development, we required experimental animals that reflect vertebrate development and are easy to observe. Zebrafish are easily obtainable and thus practical for this experiment. Zebrafish are suitable experimental animal models for this study because they are genetically homogeneous with humans and fully reflect the early developmental processes of vertebrates [12,13]. In particular, the cardiac action potential and electrocardiogram of zebrafish closely resemble those of humans, and their liver reflects basic human liver physiology [14,15]. Furthermore, zebrafish exhibit a defense mechanism against pesticides similar to that of mammals [16]. Therefore, identifying the developmental toxicity of and biological responses to bensulide in zebrafish can provide insights into the adverse effects of this pesticide on humans. Zebrafish embryos are transparent, which makes organ development easy to observe [17] and at 96 h post-fertilization (hpf), embryos complete basic cardiovascular system and complete liver development [18,19]. The development of the cardiovascular system during early embryonic development is essential for providing nutrition and removing waste for normal tissue and organ development [20]. In addition, the detoxification function of the liver mitigates the toxic effects of pesticides [21].

The main objective of this study was to identify the adverse effects of bensulide during embryogenesis and assess its potential hazards on

aquatic vertebrates and humans. The present study reveals how the malformation of zebrafish exposed to bensulide intensifies with increasing exposure concentrations. Transgenic *fli1:eGFP* and *L-fabp:dsRed* zebrafish models were utilized to examine the negative effects of bensulide, specifically on the cardiovascular system and on liver development, respectively. Cytotoxic effects such as accumulation of reactive oxygen species (ROS) and apoptosis were identified. Furthermore, changes in gene transcription associated with the malformations and cytotoxic effects caused by bensulide were analyzed. These findings could provide valuable insights into the underlying toxic mechanisms of bensulide.

## 2. Materials and methods

### 2.1. Maintenance and collection of zebrafish embryos

Wild-type (WT; AB-type) and transgenic *fli1:eGFP* and *L-fabp:dsRed* adult zebrafish were obtained from the Zebrafish Center for Disease Modeling (Chungnam National University, Republic of Korea). Transgenic *fli1:eGFP* and *L-fabp:dsRed* induce specific fluorescent signals in the cardiovascular system and liver, respectively, thereby facilitating the visualization of each organ during development. Adult zebrafish were fed thrice daily with Gemma Micro 300 ZF (Skretting, Stavanger, Norway). A water recirculating system equipped with a UV filter and maintained at a 12 h dark/light cycle at 28.5 °C was used for maintaining adult zebrafish. Breeding boxes were prepared overnight to collect embryos, with one pair of adult male and female zebrafish housed separately. The following morning, the partition separating the fish was removed and mating of the zebrafish was initiated. After fertilization, eggs were washed twice with embryo medium and incubated at 28 °C in an incubator.

### 2.2. Bensulide exposure

Bensulide (purity ≥ 95%; Catalog No. 31469, Sigma-Aldrich, Missouri, USA) was dissolved in dimethyl sulfoxide (DMSO) to create a 10 g/L bensulide stock solution. The bensulide stock solution was further diluted in embryo medium containing 0.003% 1-phenyl-2-thiourea (PTU) for zebrafish exposure. Eight hpf, WT, and transgenic zebrafish embryos were exposed to different concentrations of bensulide. A total of 36 embryos (12 embryos/well) were incubated at 28 °C in an incubator with 1.3–1.4 mL of bensulide solution. The control group received an equivalent amount of DMSO as the experimental group's highest bensulide concentration. New bensulide solutions were prepared, and living embryos were transferred to each new solution every 24 h to prevent contamination.

### 2.3. Analysis of toxicological alteration in bensulide-exposed zebrafish

The lethal effects of bensulide on zebrafish were determined at various concentrations (0, 0.5, 1, 2, 5, 8, 10, and 15 mg/L) at 96 hpf. A Quest Graph™ LC<sub>50</sub> calculator (AAT Bioquest, Inc., Sunnyvale, CA, USA) was used to determine the LC<sub>50</sub>. Subsequent experiments were performed using bensulide concentrations of 0, 1, 2, and 3 mg/L. The hatching rates were identified at each time point (48, 72, and 96 hpf), and the heart rate of the zebrafish larvae was measured for 1 min at 96 hpf. To identify morphological alterations caused by bensulide-associated toxic effects, zebrafish larvae were anesthetized with ethyl 3-aminobenzoate methanesulfonate (Tricaine; Catalog No. E10521, Sigma-Aldrich). Anesthetized larvae were fixed on glass slides with 3% methylcellulose (Catalog No. M0512; Sigma-Aldrich) and bright-field images were captured using a Leica DM 2500 microscope (Leica Microsystems, Wetzlar, Germany). Body size, body length, yolk sac size, eye size, and inner ear size were analyzed using the ImageJ software (National Institutes of Health, Bethesda, MD, USA). Experiments were performed in triplicate, and 14 zebrafish larvae were randomly selected

**Table 1**

The specific primer set for RT-qPCR experiment.

Gene	GenBank accession No.		Primer sequence (5' - 3')
<i>gapdh</i>	BC083506.1	F	5'-TGC TGG TAT TGC TCT CAA CG-3'
		R	5'-GCC ATC AGG TCA CAT ACA CG-3'
<i>tp53</i>	NM_001271820.1	F	5'-GCT TGT CAC AGG GGT CAT TT -3'
		R	5'-ACA AAG GTC CCA GTG GAG TG -3'
<i>ccne1</i>	NM_130995.1	F	5'-CGC AGT ATG CAT CAG AAA GC-3'
		R	5'-TCC ATA ACG CGT GTA TCT CG-3'
<i>ccnd</i>	NM_131025.4	F	5'-TCT CAT CCC AGA ACC TCA CC-3'
		R	5'-CTC GAT CTG TTC CTG ACA CG-3'
<i>cdk2</i>	NM_213406.1	F	5'-GAT CGG AGA GGG AAC ATA CG-3'
		R	5'-GCA GAG AGA TCT CAC GAA TGG-3'
<i>cdk6</i>	NM_001144053.1	F	5'-GGT GCA GAC TGA GGA AGA GG-3'
		R	5'-TCC TGG AAA CTG TGC ATA CG-3'
<i>sox10</i>	NM_131875.1	F	5'-TAA CAC TGC CGC ACT ACA GC-3'
		R	5'-TAG GAG AAG GCG GAG TAG AGG-3'
<i>erbB2</i>	NM_200119.2	F	5'-GAG AAC ACC TCA CCC AAA GC-3'
		R	5'-AGA CAG ATT CCC AGC AAA CG-3'
<i>erbB4a</i>	NM_001143751.1	F	5'-GAA AGC ACT GGA CCA AAA GC-3'
		R	5'-AAA AGA CGC ACC AGA TGA GG-3'
<i>erbB4b</i>	XM_009304874.3	F	5'-CAT CAA GGC CGA CTT AAA GG-3'
		R	5'-TCC GGG TTG TGA AGA GTA GC-3'
<i>gja1b</i>	NM_131038.1	F	5'-CAG GCT AAT GAG CAG AAT TGG-3'
		R	5'-TGC ATG TGA ATT GGA GAT GG-3'
<i>bif1.1</i>	XM_017352950.2	F	5'-AAC CCT GCA GAA TCC AAC AG-3'
		R	5'-TTC GAG CAG CTG AAA GAT CC-3'
<i>spaw</i>	NM_180967.2	F	5'-CCA GCC AGT TTT ATC CAA GG-3'
		R	5'-TGT GCA ATC AAG CTC AGG AC-3'
<i>actc1b</i>	NM_131591.1	F	5'-GGG TCA GAA GGA CAG CTA CG-3'
		R	5'-GCC AGA TCT TCT CCA TGT CG-3'
<i>actc2</i>	NM_001002066.1	F	5'-GCG GCT ACT CTT TTG TGA CC-3'
		R	5'-AGA AGA GGA AGC AGC AGT GG-3'
<i>fn1a</i>	NM_131520.2	F	5'-CGA GCC GCT AGT CTA CAT CC -3'
		R	5'-CTT CTT GAC CCT CGT TGA CC-3'
<i>fn1b</i>	XM_009305554.3	F	5'-TCA ATA CAA GCT CCC CAA CC-3'
		R	5'-TGA ATC GAG GAG CAT TAC CC-3'
<i>rac1b</i>	NM_001039818.1	F	5'-GTC CGT GCA AAG TGG TAT CC-3'
		R	5'-TCT CAA TGG TGT CCT TGT CG-3'
<i>bmp4</i>	NM_131342.2	F	5'-GAG ACA TGC GCT GTA TGT GG-3'
		R	5'-TGG TGG AGT TGA GAT GAT CG-3'
<i>cmcl1</i>	NM_131692.2	F	5'-AGA TGT GAT GAG GGC TCT GG-3'
		R	5'-GGC AGG AAC GTC TCA AAC AG TC-3'
<i>vegfaa</i>	AF016244.1	F	5'-AAA AGA GTG CGT GCA AGA CC-3'
		R	5'-GAG CGC CTC ATC ATT ACA GC-3'
<i>vegfab</i>	NM_001328597.1	F	5'-GCG AAA GGG AAA GAA AAA CC-3'
		R	5'-GCT GAA GTT AGG CAG GAT GG-3'
<i>vegfc</i>	AF466147.1	F	5'-GAT GTG GGG AAA GAG TTT GG-3'
		R	5'-TGA TGT TCC TGC ACT GAA GC-3'
<i>vegfd</i>	NM_001040178.1	F	5'-TCT GAT GTT GAC CGA ATA CCC-3'
		R	5'-GGC TGC ATA TCG AGT TGA CC-3'
<i>flt4</i>	AY833404.1	F	5'-TCA CAA CTG GAT GGA TTT GG-3'
		R	5'-GCC GAC AGT CTT TTC TTT GC-3'
<i>vli1</i>	NM_200238.1	F	5'-ACC TCT ATG CAT GCC AGA CC-3'
		R	5'-CTC CAC ACC TCT GCT TCT CC-3'
<i>pdgfra</i>	NM_131459.2	F	5'-CTC AGA CAT CGG AGG AAA GC-3'
		R	5'-CAG GTC TCC TGA GTC CAA GC-3'
<i>fgfr1</i>	NM_001309399.1	F	5'-GTT GAC GGA GAA CAC ACA CG-3'
		R	5'-GTT GAG TCC CTG AGC AAA GC-3'
<i>fgfr4</i>	NM_131430.1	F	5'-AAT GCT GGC TGG AGT TAT GG-3'
		R	5'-ACC ACT TGA CCA AAG CAA CC-3'
<i>kdr</i>	NM_001024653.2	F	5'-CTT GGC AGC CAG AAA TAT CC-3'
		R	5'-GAC GAG CAT CTC CTT TAC GG-3'
<i>kdr1</i>	NM_131472.1	F	5'-CCT GAT CCA CAA CTG CTT CC-3'
		R	5'-CAC AGC ACT CAA TGC GTA CC-3'
<i>hdac1</i>	NM_173236.1	F	5'-ATA TTG GTG CAG GCA AGG GG-3'
		R	5'-CAC TGG GCT GGT ACA TCT CC-3'
<i>hdac3</i>	NM_200990.1	F	5'-GTT TTC AAA CCC TAC AAG GC-3'
		R	5'-TGT TTG GAC TGA CCT TCT GC-3'
<i>wnt2bb</i>	NM_001044344.1	F	5'-GCC AAA GCC TTC ATA GAT GC-3'
		R	5'-CGC TTT ACA GCC ATT CTT CC-3'
<i>wnt8a</i>	NM_130946.3	F	5'-AAA CCT CAG CAT GGG ACT AC-3'
		R	5'-TCT ACT TTC AGG CCA CAT TCG-3'
<i>prox1</i>	NM_131405.2	F	5'-CGC TCT GAT GGA ATG GAC AA-3'
		R	5'-CTC TGC TCC CGA ATA AGT GC-3'
<i>myp1</i>	NM_001003870.2	F	5'-CTG GAG CCT GAG AAG ACT GC-3'

(continued on next page)

**Table 1** (continued)

Gene	GenBank accession No.		Primer sequence (5' - 3')
<i>gata6</i>	NM_001326364.1	R F	5'-TTC CTC CTC TTC CTC ACT CG-3' 5'-AAG TGG ATC TTA CCC GAG CC-3'
<i>fabp2</i>	NM_131431.1	R F	5'-CAG CAT GGA GTT CTC GAA GG-3' 5'-ACT TTA CTC TGG GCG TCA CC-3'
<i>bmp6</i>	NM_001013339.1	F R	5'-TAC CTT TCC GTT GTC CTT GC-3' 5'-TGC AGA TCA GTG TGG AGA CC-3'
<i>sod2</i>	NM_199976.1	F R	5'-GAC CGG GAA GTT CTG ATA CG-3' 5'-AAC CCA AGT CTC CCT TCA GC-3'
<i>cat</i>	NM_130912.2	F R	5'-TGA AAT GAG CCA AAG TCA CG-3' 5'-GGC AAC TGG GAT CTT ACA GG-3'
<i>gpx1</i>	NM_001007281.2	F R	5'-AGC TCC AAA AAT CCC AAA CC-3' 5'-ACC TGT CCG CGA AAC TAT TG-3'
<i>cox2a</i>	NM_153657.1	F R	5'-TGA CTG TTG TGC CTC AAA GC-3' 5'-ACT ACC CCT GAG CTT CTC ACA-3'
<i>cox2b</i>	NM_001025504.2	F R	5'-GAT GCT GTT GAT GAT ATC CCA GAT TG-3' 5'-GGC TCA TCC TTA TTG GTG AGA CTA T-3'
<i>cxcl-clc</i>	NM_001115060.1	F R	5'-TCG GGA TCA AAC TTG AGC TTA AAA TA-3' 5'-TCA TCT CTC GTG AAT CGT GCT -3'
<i>il1b</i>	NM_212844.2	F R	5'-TTC AGC GAG TCC GTG TTA TT -3' 5'-AGA TGG TGG AGA TGG ACA GG-3'
<i>il6</i>	JN698962.1	F R	5'-TCT CGT CTT TGG ATG GAA GC-3' 5'-GGT GAG AGA CGG AGA GAT GGA T-3'
<i>il10</i>	BC163038.1	F R	5'-CAC GCT GGA GAA GTT GAA CAG-3' 5'-TGG CTG AAA ATC AAG AAA GG-3'
<i>bcl2</i>	AY695820.1	F R	5'-AGA AGA AGC GTG AGC AGA GC-3' 5'-AGG AAA ATG GAG GTT GGG ATG-3'
<i>bcl-xl</i>	NM_131807.1	F R	5'-TGT TAG GTA TGA AAA CGG GTG GA-3' 5'-AGT TTG AGC TGC GCT ATT C-3'
			5'-CTC TCG AAG CTC TGG TAC GC-3'

for each experiment.

#### 2.4. Total RNA extraction and analysis of mRNA transcription

To isolate total RNA, zebrafish larvae ( $n = 25$ ) exposed to bensulide at 96 hpf were homogenized with 1 mL of TransZol Up reagent (TransGen Biotech, Beijing, China). Following homogenization, total RNA was extracted according to the manufacturer's guidelines. The purity and concentration of the extracted RNA were analyzed using SPECTROstar Nano (BMG Labtech, Ortenberg, Germany). AccuPower RT PreMix (Bioneer, Daejeon, Korea), random primers (Invitrogen, Massachusetts, USA), and oligo dT primers (Bioneer) were used for complementary DNA (cDNA) synthesis using reverse transcription PCR. RT-qPCR was performed using a StepOnePlus Real-Time PCR System (Applied Biosystems, Foster City, CA, USA) with cDNA, SYBR Green (Sigma-Aldrich), ROX reference dye (Invitrogen), and a specific primer set (Table 1). The level of mRNA transcription was analyzed using the  $2^{-\Delta\Delta CT}$  method [21]. A Python program was used with the Seaborn library to create a heatmap. The color of the heatmap represents the fold change in gene expression levels in the bensulide-treated group compared to those in the vehicle-treated group.

#### 2.5. Observation of the cardiovascular systems and liver development using transgenic zebrafish

The transgenic zebrafish models *fli1:eGFP* and *L-fabp:dsRed* were used to observe the toxic effects of bensulide on the cardiovascular system and liver development. In *fli1:eGFP* transgenic zebrafish, enhanced green fluorescent protein (eGFP) is expressed by the *fli1* promoter, and the cardiovascular system is labeled with green fluorescence. In *L-fabp:dsRed* transgenic zebrafish, the red fluorescent protein (dsRed) was expressed under the control of *L-fabp* promoter, and the liver was tagged with red fluorescence. Transgenic zebrafish embryos were exposed to the bensulide solution from 8 to 96 hpf. Fluorescence inversion microscopy was used to observe and capture fluorescent images of transgenic zebrafish. The captured images were analyzed using the ImageJ software. Experiments were performed in triplicate, and 14

zebrafish larvae were randomly selected for each experiment.

#### 2.6. Analysis of ROS accumulation in bensulide-exposed zebrafish

The 96 hpf WT larvae were stained with DCFH-DA (Sigma-Aldrich) for 1 h at 28 °C in the dark. The larvae stained with DCFH-DA were anesthetized by immersion in tricaine. After anesthetization, larvae were fixed on glass slides with 3% methylcellulose. The reactive oxygen species (ROS) in zebrafish larvae switched DCFH-DA to DCF. Green fluorescence emitted by DCF was detected using an inverted fluorescence microscope equipped with a GFP filter. ImageJ software was used to analyze the fluorescence intensity. Experiments were performed in triplicate, and 14 zebrafish larvae were randomly selected for each experiment.

#### 2.7. Analysis of apoptotic cells in bensulide-exposed zebrafish

The 96 hpf WT zebrafish larvae were stained with acridine orange dye (AO; Life Technologies, Carlsbad, CA, USA) for 1 h at 28 °C in the dark. AO-stained larvae were anesthetized using tricaine and fixed on glass slides with 3% methylcellulose. The AO-positive cells were detected and captured using an inverted fluorescence microscope equipped with a GFP filter. ImageJ software was used to analyze the fluorescence intensity. Experiments were performed in triplicate, and 14 zebrafish larvae were randomly selected for each experiment.

#### 2.8. Analysis of DNA fragmentation in bensulide-exposed zebrafish

DNA fragmentation, a hallmark of apoptosis, was analyzed in terminal deoxynucleotidyl transferase biotin-dUTP nick-end labeling (TUNEL)-positive cells. WT zebrafish larvae (96 hpf) were washed twice with 1X phosphate-buffered saline with 0.1% Tween-20 (PBST). The 4% paraformaldehyde (PAF) was added to washed larvae and incubated for 16 h at 4 °C for fixation. Following fixation, the 100% methanol was added to permeabilization and incubated for 16 h at -20 °C. Zebrafish larvae were washed with 1X PDT (1X PBST with 0.3% Triton X-100% and 1% DMSO) and incubated with an enzyme solution containing the

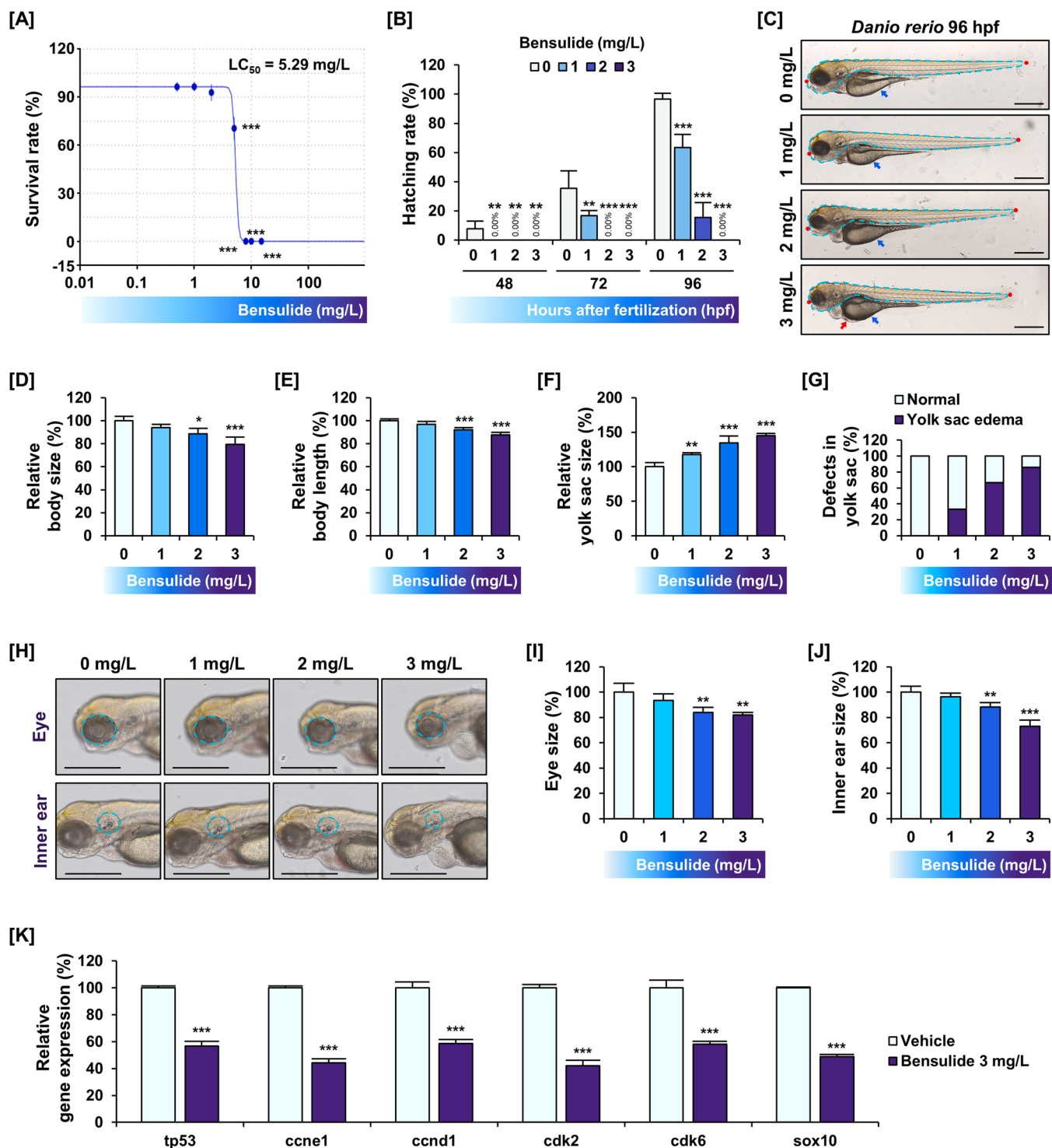


**Fig. 1.** Hazardous effects of bensulide on zebrafish larvae. [A] LC<sub>50</sub> value of zebrafish at 96 hpf was determined under various concentrations of bensulide exposure (0, 0.5, 1, 2, 5, 8, 10, and 15 mg/L). [B] The hatching rate of bensulide-exposed zebrafish larvae was identified every 24 h. [C] The bright field images of bensulide-exposed zebrafish larvae was captured at 96 hpf. The blue dotted line indicates the area of the body measured to determine body size. The red dot indicates the reference points for the body length measurement, namely the head- and tail-end reference points. The blue arrow indicates the yolk sac, while the red arrow indicates the yolk sac edema. Scale bars correspond to 500 µm. [D-G] The malformation of zebrafish larvae was observed. [D] Body size, [E] body length, [F] size of yolk sac, and [G] defects in yolk sac were analyzed. [H] The alteration of eye and inner ear were observed at 96 hpf zebrafish exposed to bensulide. The blue dotted line indicates each organ. Scale bars correspond to 500 µm. [I-J] The relative size of [I] eye and [J] ear was analyzed. [K] The changes in gene expression level induced by bensulide were identified. The asterisks represented significant difference: \*  $p < 0.05$ , \*\*  $p < 0.01$ , and \*\*\*  $p < 0.001$ .

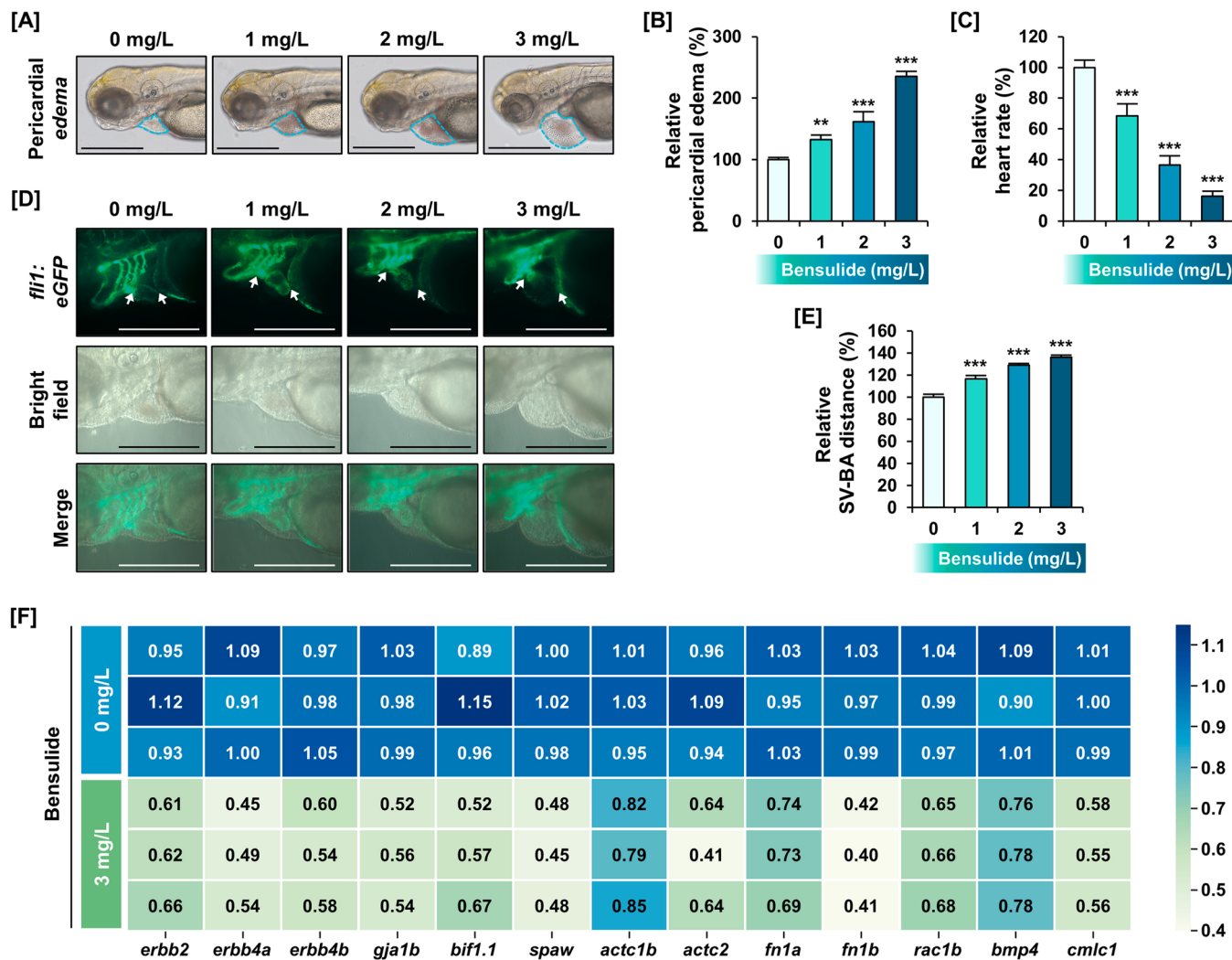


**Fig. 2.** Bensulide-associated heart defects of zebrafish larvae. [A] The bright field images showed alteration of pericardial structure. The blue dotted line indicates pericardium of zebrafish larvae. Scale bars correspond to 500  $\mu$ m. [B] The relative size of pericardial edema was analyzed. [C] The heart rate was examined for 1 min at 96 hpf zebrafish larvae. [D] Heart morphology of 96 hpf *fli1:eGFP* transgenic zebrafish was captured using green fluorescence. The white arrows indicate SV (left) and BA (right). Scale bars correspond to 500  $\mu$ m. [E] The SV-BA distance were analyzed. [F] The transcription of genes related to heart development (*erbb2*, *erbb4a*, *erbb4b*, *gja1b*, *bif1.1*, *spaw*, *actc1b*, *actc2*, *fn1a*, *fn1b*, *rac1b*, *bmp4*, and *cmhc1*) was analyzed. The significant difference is represented by asterisks: \*\*  $p < 0.01$ , and \*\*\*  $p < 0.001$ .

TUNEL labeling solution. After incubation, larvae were stained with 3  $\mu$ g/mL DAPI for 15 min. TUNEL- and DAPI-stained larvae were fixed on glass slides with 3% methylcellulose and detected using a confocal laser scanning microscope LSM700 (ZEISS, Jena, Germany). ImageJ software was used to analyze the fluorescence intensity.

## 2.9. Statistical analysis

SAS software (SAS Institute, Cary, NC, USA) was used to identify statistically significant differences between the control and experimental groups. The analysis also included ANOVA (a one-way analysis of variance) with the general linear model (PROG-GLM). Tukey's test was used for multiple comparisons during statistical analysis. All results were presented as the mean with standard deviation. Statistical significance was exhibited by  $p$ -values  $< 0.05$  and were identified with an asterisk (\*).

## 3. Results

### 3.1. Developmental malformations in bensulide-exposed zebrafish embryos

The survival rate of zebrafish embryos after bensulide exposure was calculated at 96 hpf for each concentration (0, 0.5, 1, 2, 5, 8, 10, and 15 mg/L). The LC<sub>50</sub> was determined at 5.29 mg/L concentration (Fig. 1A). Subsequent experiments were performed wherein all zebrafish survived at 96 hpf at concentrations lower than the LC<sub>50</sub> value. The relative hatchability of fertilized eggs was examined at concentrations of 0, 1, 2, and 3 mg/L (Fig. 1B). Under 3 mg/L bensulide exposure, whole-fertilized eggs did not hatch until 96 hpf. After exposure to 1 mg/L and 2 mg/L bensulide, 66.33% ( $p < 0.001$ ) and 15.56% ( $p < 0.001$ ) of fertilized eggs, respectively, hatched at 96 hpf. Bensulide-induced malformations were observed in zebrafish larvae at 96 hpf (Fig. 1C). Decreases in body size to 79.48% ( $p < 0.001$ ) and length to 87.57% ( $p < 0.001$ ) indicated growth inhibition after exposure to 3 mg/L bensulide (Figs. 1D and 1E). Furthermore, increased bensulide concentrations led to larger yolk sacs (Fig. 1F). Bensulide increases the proportion of zebrafish with yolk sac defects to 85.71% ( $n = 42$ ) at 3 mg/L

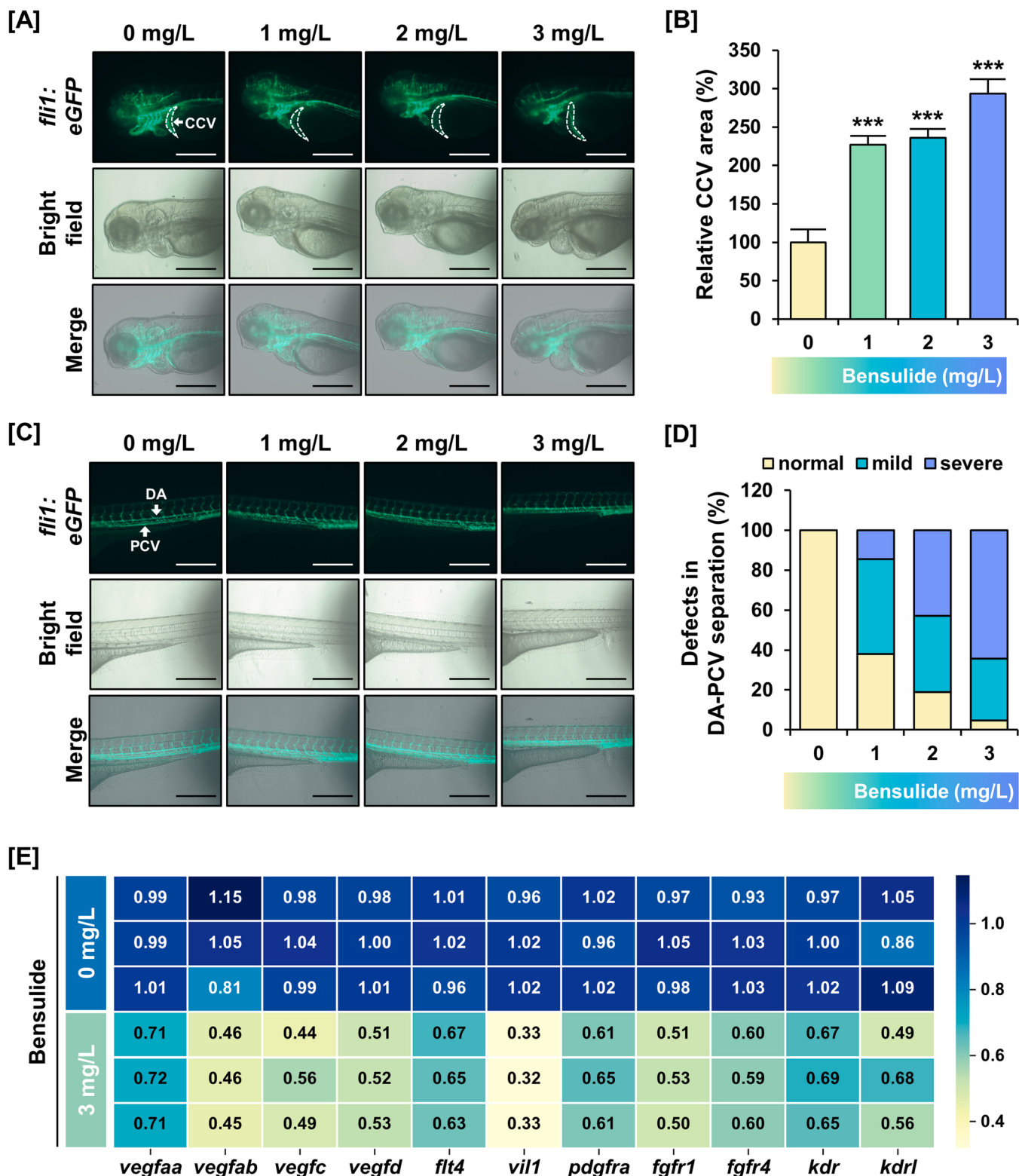


**Fig. 3.** The malformation of zebrafish vasculature induced by bensulide. [A] The hypertrophy of the CCV area of 96 hpf *fltl:eGFP* zebrafish was observed. The white dotted lines indicated CCV area. Scale bars correspond to 500  $\mu$ m. [B] The relative size of CCV area was analyzed. [C] The separation between DA and PCV was captured. Scale bars correspond to 500  $\mu$ m. [D] Depending on the severity of the DA-PCV separation defect, the zebrafish exposed to bensulide were divided into three groups: normal, mild, and severe. The percentage of each group was determined. [E] The alterations of transcription of vascular development-related genes (*vegfaa*, *vegfab*, *vegfc*, *vegfd*, *flt4*, *vil1*, *pdgfra*, *fgfr1*, *fgfr4*, *kdr*, and *kdrl*) were identified. The fold changes in gene expression levels are represented by annotations relative to the average expression level in the vehicle-treated group. Each row represents the biological triplicate experiments of both vehicle- and bensulide-treated groups. The significant difference is represented by asterisks: \*\*\*  $p < 0.001$ .

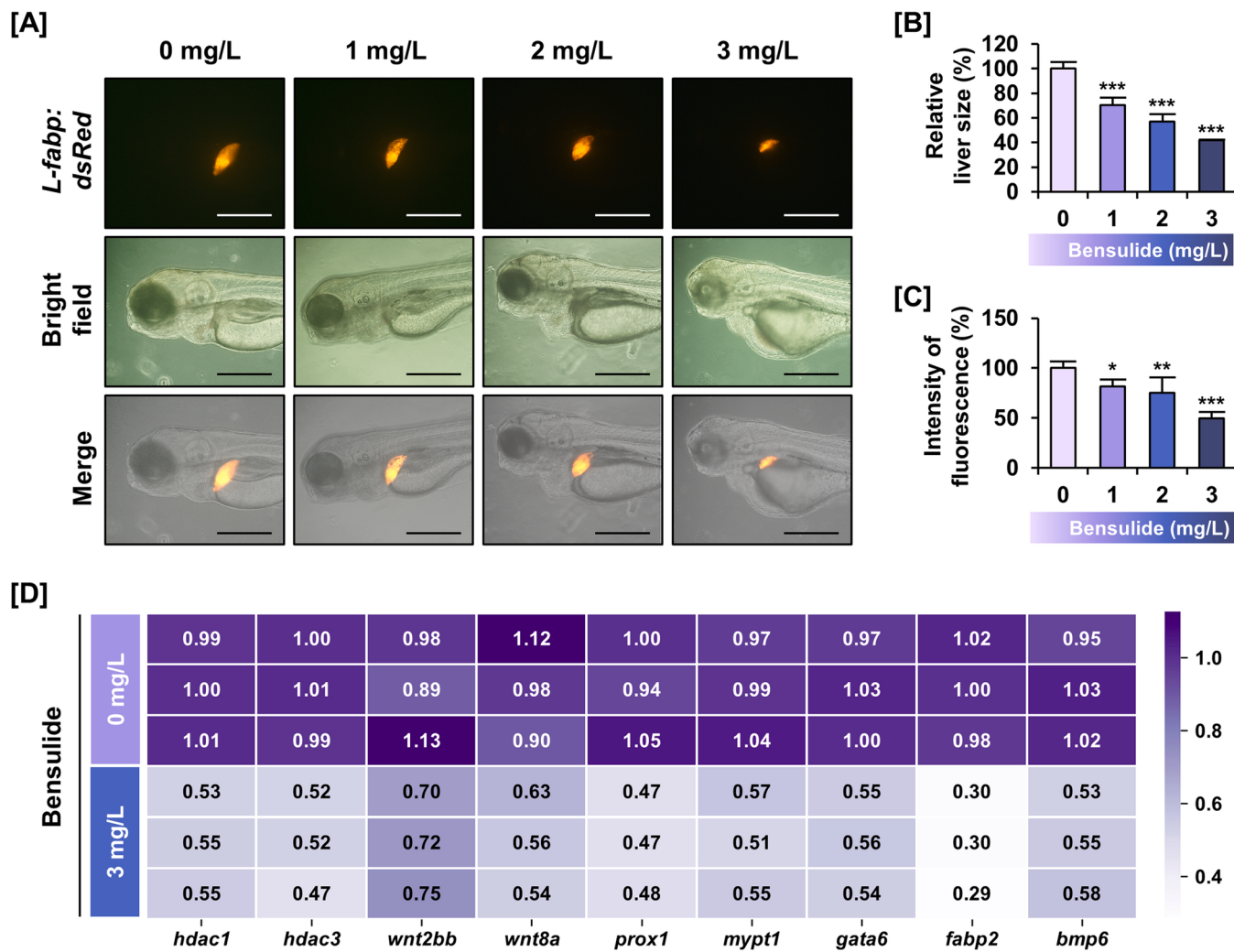


**Fig. 4.** The inhibition of liver development caused by bensulide. [A] The liver size and fluorescence intensity of *L-fabp:dsRed* transgenic zebrafish were observed. Scale bars correspond to 500  $\mu$ m. [B] The relative size of liver was analyzed. [C] The fluorescence intensity of liver in *L-fabp:dsRed* zebrafish was identified. [D] The transcription alterations of liver development-related gene (*hdac1*, *hdac3*, *wnt2bb*, *wnt8a*, *prox1*, *mypt1*, *gata6*, *fabp2*, and *bmp6*) were analyzed. The fold changes in gene expression levels compared to the average in the vehicle-treated group were presented with annotations. The biological triplicated experiments of vehicle and bensulide-treated group are represented in each row. The significant difference is represented by asterisks: \*  $p < 0.05$ , \*\*  $p < 0.01$ , and \*\*\*  $p < 0.001$ .

concentrations (Fig. 1G). The reduction in eye size to 81.96% ( $p < 0.01$ ) and inner ear size to 72.85% ( $p < 0.001$ ) following exposure to 3 mg/L bensulide indicated that it could impair the development of special sensory organs during embryonic development (Fig. 1H–J). The transcription levels of embryo development-associated genes (*tp53*, *ccne1*, *ccnd1*, *cdk2*, *cdk6*, and *sox10*) decreased after bensulide exposure at 96 hpf (Fig. 1K). These results suggest that bensulide inhibits the normal development of zebrafish embryos and can result in severe deformities as the concentration increases.

### 3.2. Heart defects in bensulide-exposed zebrafish embryos

Bensulide exposure was observed to induce heart malformations. The extent of the pericardial edema increased with increasing bensulide concentration (Fig. 2A). The relative pericardial edema sizes increased to 132.95% ( $p < 0.01$ ), 161.90% ( $p < 0.001$ ), and 235.42% ( $p < 0.001$ ) following exposure to 1, 2, and 3 mg/L bensulide, respectively (Fig. 2B). In addition, the heart rate per minute was measured to determine the effect of bensulide exposure on heart function. The relative heart rates decreased to 68.46% ( $p < 0.001$ ), 36.57% ( $p < 0.001$ ), and 16.37% ( $p < 0.001$ ) after exposure to 1, 2, and 3 mg/L of bensulide, respectively (Fig. 2C). The *fli1:eGFP* transgenic model further exhibited heart

abnormalities, such as pericardial edema. The distance between sinus venosus (SV) and bulbus arteriosus (BA) was analyzed to identify the occurrence of heart looping. Bensulide exposure increased the SV-BA distance by 116.67% ( $p < 0.001$ ), 128.98% ( $p < 0.001$ ), and 136.27% ( $p < 0.001$ ) after exposure to 1, 2, and 3 mg/L of bensulide, respectively (Figs. 2D and 2E). Heart development is regulated by the expression of various genes. Therefore, alterations in gene expression were investigated to further confirm the effects of bensulide on cardiac development. The expression levels of 13 genes (*erbb2*, *erbb4a*, *erbb4b*, *gja1b*, *bif1.1*, *spaw*, *actc1b*, *actc2*, *fn1a*, *fn1b*, *rac1b*, *bmp4*, and *cmlc1*) were reduced following bensulide treatment (Fig. 2F). Bensulide exposure may therefore hinder zebrafish heart development.

### 3.3. Vascular malformation in bensulide-exposed zebrafish embryos

Vasculogenesis and angiogenesis occur during embryogenesis to form zebrafish vasculature. The effects of bensulide on blood vessel development were observed in *fli1:eGFP* transgenic zebrafish model. The common cardinal vein (CCV), a blood vessel connected to the sinus venosus during embryogenesis, showed abnormal morphology after bensulide exposure at 96 hpf (Fig. 3A). The relative size of the CCV increased to 226.90% ( $p < 0.001$ ), 235.77% ( $p < 0.001$ ), and 293.46%

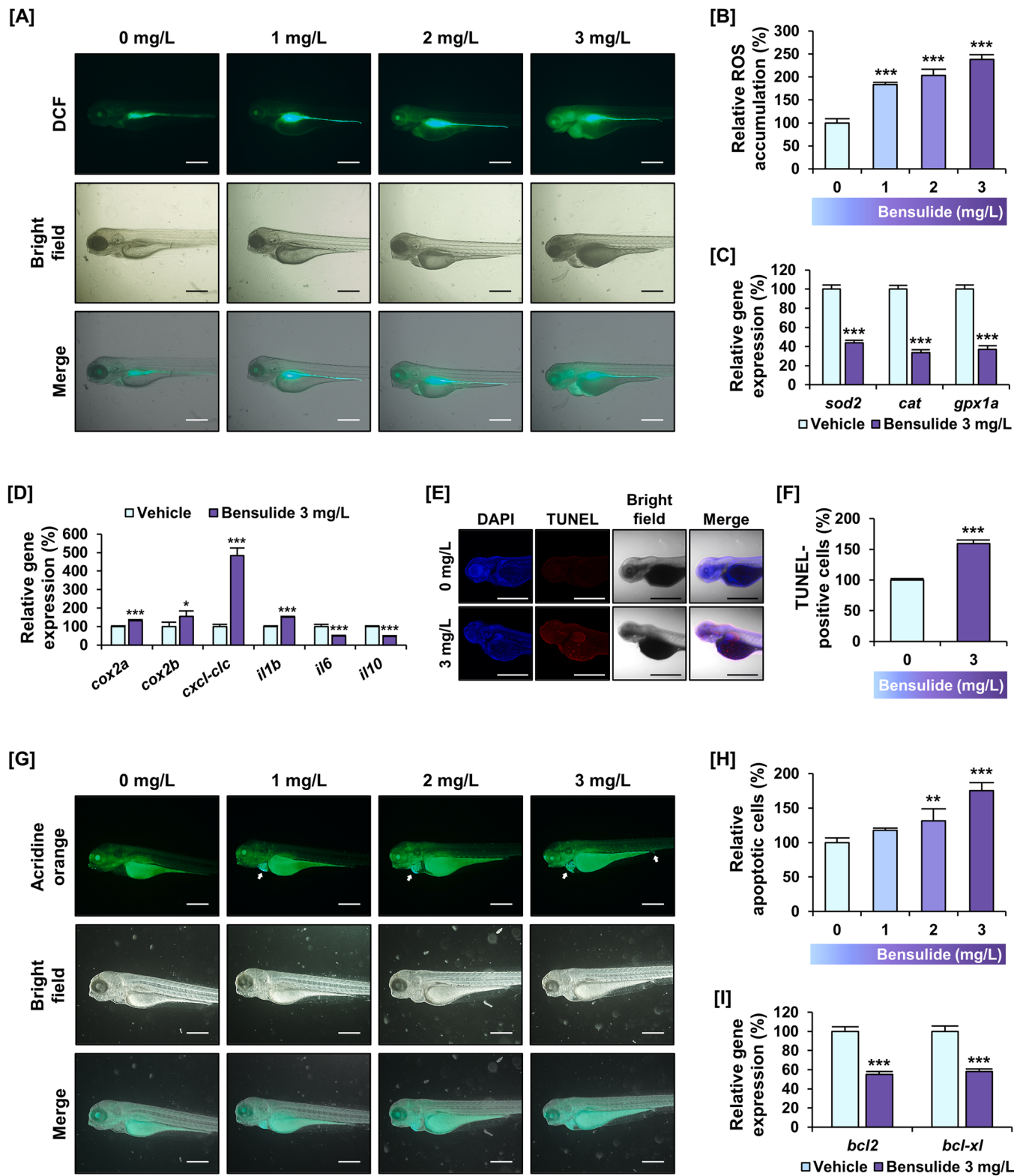


**Fig. 5.** The cytotoxic effects of bensulide including ROS accumulation and apoptosis. [A] The ROS accumulation after bensulide exposure was indicated by green fluorescence. Scale bars correspond to 500  $\mu$ m. [B] The intensity of green fluorescence was analyzed to identify the level of ROS accumulation. [C-D] The transcription of genes encoded [C] antioxidant enzyme (*sod2*, *cat*, and *gpx1a*) and [D] inflammatory cytokines (*cox2a*, *cox2b*, *cxcl-clc*, *il1b*, *il6*, and *il10*) were analyzed. [E] DNA fragmentation in apoptotic cells was visualized using TUNEL-positive apoptotic cells that emitted red fluorescence. DAPI-stained cells emitted a blue signal. Scale bars correspond to 500  $\mu$ m. [F] The percentage of apoptotic cells was determined based on the intensity of TUNEL/DAPI. [G] Apoptosis induced by bensulide was indicated by green fluorescent dots via acridine orange staining. White arrows indicate the foci of acridine orange cells. Scale bars correspond to 500  $\mu$ m. [H] The acridine orange-positive apoptotic cells were analyzed. [I] Relative changes in the expression of apoptotic genes (*bcl2* and *bcl-xl*) were identified. All fluorescent staining experiments were performed using wild-type zebrafish to avoid interference from other fluorescence signals. The significant difference is represented by asterisks: \*  $p < 0.05$ , \*\*  $p < 0.01$ , and \*\*\*  $p < 0.001$ .

( $p < 0.001$ ) after exposure to 1, 2, and 3 mg/L of bensulide, respectively (Fig. 3B). In zebrafish embryos exposed to bensulide, the dorsal aorta (DA) and posterior cardinal vein (PCV) were not properly separated (Fig. 3C). By observing the separation between the DA and PCV, zebrafish larvae were classified into normal, mild, and severe groups. We defined a defect as mild when the boundary between the DA and PCV was less distinct, and as severe when there was no visible boundary. The number of larvae in the severe group, in which DA and PCV were not separated, increased with increasing exposure to bensulide (Fig. 3D). Eleven genes related to zebrafish vascular development (*vegfaa*, *vegfab*, *vegfc*, *vegfd*, *flt4*, *vil1*, *pdgfra*, *fgfr1*, *fgfr4*, *kdr*, and *kdr1*) were downregulated (Fig. 3E), indicating that abnormal regulation of these genes may contribute to cardiovascular defects.

### 3.4. Abnormal liver development in the bensulide-exposed zebrafish embryos

The liver is the primary organ involved in the metabolism of xenobiotics including pesticides. Bensulide exposure affects hepatogenesis, the developmental process of the liver. Therefore, the *L-fabp:dsRed*

transgenic zebrafish model was used to identify the adverse effects of bensulide on liver development. Livers labeled with red fluorescence were captured (Fig. 4A) and the relative liver size decreased to 70.53% ( $p < 0.001$ ), 57.12% ( $p < 0.001$ ), and 41.98% ( $p < 0.001$ ) after exposure to 0, 1, 2, and 3 mg/L bensulide, respectively, at 96 hpf (Fig. 4B). The fluorescence signal emitted by *L-fabp*-positive cells in the liver also decreased to 81.76% ( $p < 0.05$ ), 75.29% ( $p < 0.01$ ), and 49.46% ( $p < 0.001$ ) after exposure to each bensulide concentration, respectively (Fig. 4C). Bensulide downregulated the transcription of genes related to liver development. The expression of nine genes (*hdac1*, *hdac3*, *wnt2bb*, *wnt8a*, *prox1*, *mypt1*, *gata6*, *fabp2*, and *bmp6*) was analyzed to identify the transcriptional alterations caused by bensulide that result in reduced liver development (Fig. 4D). These results imply that bensulide dysregulates the expression of liver development-related genes and induces abnormal liver development during zebrafish embryogenesis.

### 3.5. Bensulide-induced cytotoxicity in zebrafish embryos

Malformation of zebrafish embryos following exposure to bensulide at 96 hpf implied that bensulide could induce cytotoxic effects.

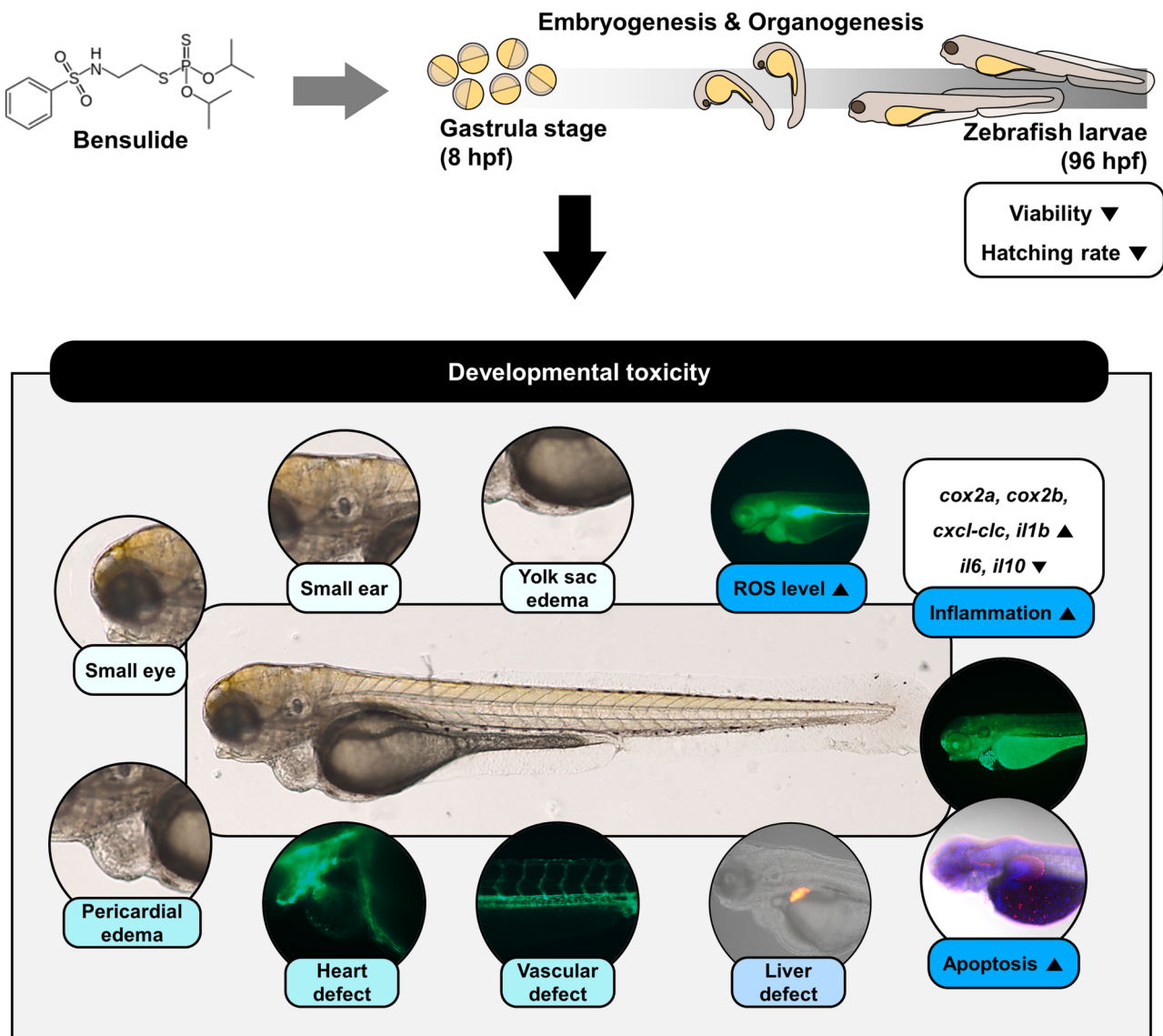


**Fig. 6.** Bensulide-caused developmental toxicity during zebrafish embryogenesis. Zebrafish embryos are exposed to bensulide from 8 hpf to 96 hpf. The bensulide induced the accumulation of ROS and apoptosis. The abnormal development of various organs are shown after bensulide exposure. Particularly, the malformation of heart, blood vessel, and liver are induced after bensulide expression.

Pesticides are associated with ROS accumulation and induction of oxidative stress [22]. Therefore, we evaluated the ability of bensulide to accumulate ROS in zebrafish embryos. ROS accumulation was detected using DCFH-DA, which produces DCF with green fluorescence in response to ROS (Fig. 5A). Bensulide exposure resulted in ROS accumulation of 183.30% ( $p < 0.001$ ), 203.62% ( $p < 0.001$ ), and 238.29% ( $p < 0.001$ ) at concentrations of 1, 2, and 3 mg/L, respectively (Fig. 5B). Antioxidant enzymes serve to eliminate ROS when there is an accumulation of ROS. However, the expression of genes encoding antioxidant enzymes, such as *sod2*, *cat*, and *gpx1a* was significantly reduced after bensulide exposure (Fig. 5C). Increased ROS levels are key signaling molecules that regulate inflammatory cytokines [23]. Bensulide exposure resulted in the upregulation of pro-inflammatory cytokines (*cox2a*, *cox2b*, *cxcl-clc* and *il1b*) and downregulation of anti-inflammatory cytokines (*il6* and *il10*) (Fig. 5D). These results showed that the increase in expression of other factors is not as dramatic as the change in *cxcl-clc*; however, it can have physiological implications. For example, only a 2-fold increase in *cox2b* mRNA caused abnormal behavior in zebrafish [24]. Increase in *il1b* mRNA also mediated inflammatory responses in zebrafish, and a 2-fold increase in *il1b* mRNA upon nanoparticle exposure induced neutrophil migration in zebrafish larvae [25]. Other studies also reported that similar changes in *il1b* mRNA levels mediated immune responses, including lymphocyte recruitment [26,27]. Additionally, the downregulation of gene expression of *il6* and *il10* have anti-inflammatory functions, suggesting that inflammatory responses could be enhanced [28]. The ROS accumulation and inflammation induced apoptosis. Therefore, apoptotic cells were detected using TUNEL staining (Fig. 5E). The percentage of TUNEL-positive cells increased to 159.33% ( $p < 0.001$ ) in the zebrafish larvae exposed to 3 mg/L bensulide (Fig. 5F). Additionally, AO staining was performed to determine the number of apoptotic cells (Fig. 5G). The number of apoptotic cells significantly increased to 131.50% ( $p < 0.01$ ) and 175.49% ( $p < 0.001$ ) after exposure to 0, 1, 2, and 3 mg/L bensulide, respectively (Fig. 5H). Exposure to 3 mg/L bensulide downregulated the expression of antiapoptotic *bcl-2* family (*bcl2* and *bcl-xl*) (Fig. 5I). Therefore, the potential cytotoxic effects of bensulide on zebrafish larvae seem to be apoptosis.

#### 4. Discussion

The premise of this study was that bensulide adversely affects early embryonic development in vertebrates. The long half-life and high absorption risk of bensulide in organisms suggest a biological risk to non-target organisms. However, developmental abnormalities and biological responses during embryogenesis after exposure to bensulide have not been reported and remain controversial. Zebrafish show a high degree of genetic homogeneity with humans and share many similarities in organ development and functions. This study aimed to identify the adverse effects of bensulide on embryogenesis and organ development, and further confirmed the transcriptional alterations caused by bensulide. These findings imply the potential hazards of bensulide in humans. Zebrafish larvae were exposed to bensulide from 8 to 96 hpf to identify the developmental toxicity of bensulide in aquatic vertebrates. Additionally, statistical significance was verified using ANOVA with PROG-GLM of all quantified data. As a large sample size could affect statistical significance, an effect size verification was conducted using Cohen's *d* value measurement [29]. All samples with statistical significance (indicated with an asterisk) had a 'very large' effect size ( $d \geq 1.3$ ). The results of our study showed that bensulide has a hazardous effect on embryogenesis. Abnormalities in zebrafish larvae caused by bensulide are schematically shown in Fig. 6.

The LC<sub>50</sub> value of bensulide was calculated in 96 hpf zebrafish larvae. Subsequent experiments were conducted with bensulide at concentrations up to 3 mg/L. We identified a decreased hatching rate with an increase in bensulide concentration. In addition, malformations were observed in organs, such as the yolk sac, eyes, and inner ear. The

higher the exposure concentration of bensulide, the more intense the abnormalities identified. For normal gastrulation and organogenesis, the cell cycle must be closely during embryogenesis for normal gastrulation and organogenesis [30]. Cell cycle dysregulation can lead to abnormal cellular development. Therefore, the expression of cell cycle-related genes (*tp53*, *ccne1*, *ccnd1*, *cdk2*, and *cdk6*) was analyzed to identify the genetic alterations underlying bensulide-induced deformities. We propose that the malformation of zebrafish larvae exposed to bensulide was caused by the inhibition of cell cycle regulatory genes. Dysregulation of cell cycle regulatory genes can affect angiogenesis [31], heart formation [32], and liver development [33]. Additionally, the expression of *sox10* gene, a key factor in ear development [34], was analyzed. Our study showed that bensulide exposure caused a minor downregulation in the inner ear and *sox10*. These findings align with previous research that has linked mutations in *sox10* genes with small inner ears [34,35].

Fluorescent-labeled transgenic models were used to identify malformations of the cardiovascular system and liver induced by bensulide. First, defects in the cardiovascular system caused by bensulide were evaluated using the *fli1:eGFP* zebrafish model. During heart development in zebrafish, myocardial cells migrate into the heart tube and initiate left-right asymmetric patterning [36]. These processes are regulated by *spaw* and *bmp4* signals [37,38]. The *erbB* family regulates trabeculation in the heart tube [39] and failure of trabeculation causes cardiomyopathy and heart defects [40]. Additionally, the cardiac conduction system and contraction are associated with genes encoding actin alpha cardiac muscles (*actc1b* and *actc2*), cardiac myosin light chain-1 (*cmlc1*), and *gia1b* [41–43]. In addition, the development of blood vessels in zebrafish during embryogenesis is influenced by various genes along with heart development. The vasculogenesis and angiogenesis are mediated by the vascular endothelial growth factor (VEGF) signals [44]. Genes of the VEGF family (*vegfaa*, *vegfbab*, *vegfc*, and *vegfd*) and their receptors (*flt4* and *kdr*) are tightly regulated during normal vasculature development [45,46]. This study showed that bensulide caused abnormal morphology and functional defects in the cardiovascular system by inhibiting gene expression. These findings are consistent with previous studies on the role of genes in the formation of the cardiovascular system. Therefore, we suggest that bensulide might cause heart and vascular defects by inhibiting the expression of related genes. Liver growth inhibition was also observed in 96 hpf zebrafish exposed to bensulide. During hepatogenesis, endoderm cells differentiate into hepatoblasts, and this process is regulated by both GATA6 and mesodermal Wnt signal, including *wnt2bb* and *wnt8a* [47–49]. The migration of hepatoblasts is regulated by expression of *prox1* and *mypt1* [50,51]. The expression of *prox1* is regulated by *hdac1* and *hdac3* [52,53]. The regulation of these genes is closely related to normal liver development. For example, deletion of Wnt signaling disrupts hepatic morphogenesis [54]. Additionally, the ablation of *prox1* expression causes defects in hepatocyte morphology and reduces liver development-related gene expression [55]. This study confirmed that bensulide downregulates related genes (*gata6*, *wnt2bb*, *wnt8a*, *prox1*, *mypt1*, *hdac1*, and *hdac3*) and results in the development of a smaller liver than in normal zebrafish during embryogenesis. These results are consistent with previous research that showed a reduction in liver size can result from a malfunction in the expression of related genes.

Finally, the cytotoxic effects of bensulide on zebrafish larvae were evaluated. The ROS accumulation can be generally induced by pesticides [22]. Typically, the ROS produced in vivo are neutralized by the body's antioxidant systems to maintain an appropriate level that does not cause adverse effects. Members of the superoxide dismutase (SOD) family, catalase, and glutathione peroxidase act as key enzymes that reduce high ROS levels in zebrafish [56]. Increased ROS levels can cause inflammation via oxidative stress owing to ROS accumulation [57]. Our findings suggest that bensulide might control the expression of inflammatory mediators by altering mRNA expression. However, confirming these results necessitates determination of the protein expression level through western blotting or ELISA. Following bensulide exposure, ROS

levels increase throughout the body of zebrafish embryos. Oxidative stress and inflammation caused by ROS activate cell death signaling [58]. Therefore, apoptosis was also observed in the zebrafish larvae exposed to bensulide. Exposure to bensulide resulted in an increase in apoptotic cells throughout the zebrafish embryos, which corresponded to the accumulation of ROS. Bcl-2 and Bcl-XL, owing to their pro-apoptotic signal inhibiting ability, act as powerful anti-apoptotic factors [59]. However, bensulide inhibits the transcription of *bcl2* and *bcl-xl* involved in cell survival signaling and induce apoptosis. The findings of the present study demonstrate that bensulide inhibits the expression of antioxidants during zebrafish embryogenesis, leading to ROS accumulation and inflammatory responses, further causing apoptosis. These results correspond well with those of previous studies on the correlation between antioxidant activity, inflammation, and apoptosis. In addition, increased oxidative stress mediates abnormal embryonic development of the eyes, heart, blood vessels, and liver [60]. Therefore, we suggest that ROS accumulation and increased oxidative stress might be the key mechanisms underlying bensulide toxicity.

This study clarified the adverse effects of bensulide on zebrafish embryonic development. This is the first study on bensulide to report developmental toxicity and biological responses on genetic and cellular levels. These results suggest that the exposure of zebrafish to bensulide at the gastrula stage can potentially induce various defects in the organs via oxidative stress. We suggest that the developmental toxicity of bensulide detected in this study may also occur in humans, considering that zebrafish and humans share a genetically homogenous background and possess similar mechanisms of organ development and cell signaling systems, such as inflammatory cytokines. In addition, this study provides an outline for identifying the developmental toxicity of other xenobiotics, including herbicides. However, the present study did not provide information on bensulide metabolism. Details on its mode of action, binding ability to intracellular signaling molecules, and production of metabolites requires further investigation. In addition, some organs have been targeted to address developmental toxicity. Therefore, further research is required to find the major target organ and mechanisms of action of bensulide.

## 5. Conclusions

Collectively, these results demonstrate the developmental toxicity of bensulide in zebrafish. The developmental toxicity of bensulide is based on the oxidative stress induced by excessive ROS accumulation. Bensulide was observed to induce inflammatory response and apoptosis. It causes the abnormal expression of genes related to normal growth, cardiovascular system development, and hepatogenesis. Defects in the cardiovascular system and liver have been identified owing to dysregulated gene expression. To the best of our knowledge, this is the first study to investigate the biological responses to the toxic effects of bensulide during development. In this study, the developmental toxicity of bensulide was evaluated in some organs; however, did not consider the metabolic processes of bensulide in zebrafish embryos. Therefore, further studies on metabolic processes and adverse effects on other organs are required. Moreover, because zebrafish and humans have a similar developmental process with high genetic homogeneity, it is necessary to investigate the adverse effects of bensulide on human embryonic development.

## CRediT authorship contribution statement

**Miji Kim:** Investigation, Methodology, Software, Writing – original draft. **Garam An:** Investigation, Methodology, Software, Writing – original draft. **Junho Park:** Investigation, Writing – original draft. **Whasun Lim:** Conceptualization, Validation, Investigation, Methodology, Software, Writing – original draft, Writing – review & editing. **Gwonhwa Song:** Conceptualization, Validation, Supervision, Writing – original draft, Writing – review & editing.

## Environmental Implication

Bensulide is the organophosphate herbicide that has been used in weed control in conventional agriculture with a high risk of accumulation in aquatic systems. Results of this study clarified that bensulide interrupted development in zebrafish. Following bensulide exposure, genes related to the cardiovascular system and liver development were dysregulated in various developmental stages. Bensulide exerts toxic effects via reactive oxygen species accumulation, inflammation, and apoptosis. This study provides new insights into the risk assessment of bensulide using a zebrafish transgenic model by estimating abnormal morphogenesis, cell cycle arrest, apoptosis, transcriptional profiling, and cardiovascular toxicity.

## Declaration of Competing Interest

The authors declare that they have no known competing financial interests or personal relationships that could have appeared to influence the work reported in this paper.

## Data Availability

The data that has been used is confidential.

## Acknowledgements

This research was supported by the National Research Foundation of Korea (NRF) grant funded by the Korea government (MSIT) (grant number: 2021R1A2C2005841 & 2021R1C1C1009807). This research was also supported by the Health Fellowship Foundation. This research was supported by Basic Science Research Program through the NRF funded by the Ministry of Education (grant number: 2019R1A6A1A10073079). The authors thank Sohyung Kim (Seoul National University, Korea) for technical assistance in data visualization.

## Appendix A. Supporting information

Supplementary data associated with this article can be found in the online version at doi:10.1016/j.jhazmat.2023.131577.

## References

- [1] Cooper, J., Dobson, H., 2007. The benefits of pesticides to mankind and the environment. *Crop Prot* 26, 1337–1348.
- [2] Aktar, M.W., Sengupta, D., Chowdhury, A., 2009. Impact of pesticides use in agriculture: their benefits and hazards. *Inter Toxicol* 2, 1–12.
- [3] Antonious, G.F., 2010. Mobility and half-life of bensulide in agricultural soil. *J Environ Sci Health B* 45, 1–10.
- [4] I. Bensulide, O. Pesticides, Reregistration Eligibility Decision for Bensulide, (2006).
- [5] Menges, R., Hubbard, J., 1970. Selectivity, movement, and persistence of soil-incorporated herbicides in carrot plantings. *Weed Sci* 18, 247–252.
- [6] Haith, D.A., Rossi, F.S., 2003. Risk assessment of pesticide runoff from turf. *J Environ Qual* 32, 447–455.
- [7] Lopez-Garcia, M., Romero-Gonzalez, R., Garrido, A., 2019. Frenich, Monitoring of organophosphate and pyrethroid metabolites in human urine samples by an automated method (TurboFlow) coupled to ultra-high performance liquid chromatography-Orbitrap mass spectrometry. *J Pharm Biomed Anal* 173, 31–39.
- [8] Zilkah, S., Osband, M.E., McCaffrey, R., 1981. Effect of inhibitors of plant cell division on mammalian tumor cells in vitro. *Cancer Res* 41, 1879–1883.
- [9] McCorle, F.M., Chambers, J.E., Yarbrough, J.D., 1977. Acute toxicities of selected herbicides to fingerling channel catfish, *Ictalurus punctatus*. *Bull Environ Contam Toxicol* 18, 267–270.
- [10] Kleinstreuer, N.C., Judson, R.S., Reif, D.M., Sipes, N.S., Singh, A.V., Chandler, K.J., Dewoskin, R., Dix, D.J., Kavlock, R.J., Knudsen, T.B., 2011. Environmental impact on vascular development predicted by high-throughput screening. *Environ Health Perspect* 119, 1596–1603.
- [11] Shellenberger, T.E., Newell, G.W., Bridgman, R.M., Barbaccia, J., 1965. A subacute toxicity study of N-(2-mercaptoethyl) benzene-sulfonamide S-(O,O-diisopropyl phosphorodithioate) and phthalimidomethyl-O,O-dimethyl phosphorodithioate with Japanese quail. *Toxicol Appl Pharm* 7, 550–558.
- [12] Howe, K., Clark, M.D., Torroja, C.F., Torrance, J., Berthelot, C., Muffato, M., Collins, J.E., Humphray, S., McLaren, K., Matthews, L., McLaren, S., Sealy, I., Caccamo, M., Churcher, C., Scott, C., Barrett, J.C., Koch, R., Rauch, G.J., White, S.,

- [1] Chow, W., Kilian, B., Quintais, L.T., Guerra-Assuncao, J.A., Zhou, Y., Gu, Y., Yen, J., Vogel, J.H., Eyer, T., Redmond, S., Banerjee, R., Chi, J., Fu, B., Langley, E., Maguire, S.F., Laird, G.K., Lloyd, D., Kenyon, E., Donaldson, S., Sehra, H., Almeida-King, J., Loveland, J., Trevanion, S., Jones, M., Quail, M., Willey, D., Hunt, A., Burton, J., Sims, S., McLay, K., Plumb, B., Davis, J., Cleee, C., Oliver, K., Clark, R., Riddle, C., Elliot, D., Threadgold, G., Harden, G., Ware, D., Begum, S., Mortimore, B., Kerr, G., Heath, P., Phillimore, B., Tracey, A., Corby, N., Dunn, M., Johnson, C., Wood, J., Clark, S., Pelan, S., Griffiths, G., Smith, M., Glithero, R., Howden, P., Barker, N., Lloyd, C., Stevens, C., Harley, J., Holt, K., Panagiotidis, G., Lovell, J., Beasley, H., Henderson, C., Gordon, D., Auger, K., Wright, D., Collins, J., Raisen, C., Dyer, L., Leung, K., Robertson, L., Ambridge, K., Leongamornlert, D., McGuire, S., Gilderthorpe, R., Griffiths, C., Manthravadi, D., Nichol, S., Barker, G., Whitehead, S., Kay, M., Brown, J., Murnane, C., Gray, E., Humphries, M., Sycamore, N., Barker, D., Saunders, D., Wallis, J., Babbage, A., Hammond, S., Mashreghi-Mohammadi, M., Barr, L., Martin, S., Wray, P., Ellington, A., Matthews, N., Ellwood, M., Woodmansey, R., Clark, G., Cooper, J., Tromans, A., Grafham, D., Skuce, C., Pandian, R., Andrews, R., Harrison, E., Kimberley, A., Garnett, J., Fosker, N., Hall, R., Garner, P., Kelly, D., Bird, C., Palmer, S., Gehring, I., Berger, A., Dooley, C.M., Ersan-Urun, Z., Eser, C., Geiger, H., Geisler, M., Karotki, L., Kirn, A., Konantz, J., Konantz, M., Oberlander, M., Rudolph-Geiger, S., Teucke, M., Lanz, C., Raddatz, G., Osoegawa, K., Zhu, B., Rapp, A., Widaa, S., Langford, C., Yang, F., Schuster, S.C., Carter, N.P., Harrow, J., Ning, Z., Herrero, J., Searle, S.M., Enright, A., Geisler, R., Plasterk, R.H., Lee, C., Westerfield, M., de Jong, P.J., Zon, L.I., Postlethwait, J.H., Nusslein-Volhard, C., Hubbard, T.J., Roest Crollius, H., Rogers, J., Stemple, D.L., 2013. The zebrafish reference genome sequence and its relationship to the human genome. *Nature* 496, 498–503.
- [13] Veldman, M.B., Lin, S., 2008. Zebrafish as a developmental model organism for pediatric research. *Pedia Res* 64, 470–476.
- [14] Nemtsas, P., Wettwer, E., Christ, T., Weidinger, G., Ravens, U., 2010. Adult zebrafish heart as a model for human heart? An electrophysiological study. *J Mol Cell Cardiol* 48, 161–171.
- [15] Wilkins, B.J., Pack, M., 2013. Zebrafish models of human liver development and disease. *Compt Physiol* 3, 1213–1230.
- [16] McGrath, P., Li, C.Q., 2008. Zebrafish: a predictive model for assessing drug-induced toxicity. *Drug Discov Today* 13, 394–401.
- [17] Antinucci, P., Hindges, R., 2016. A crystal-clear zebrafish for in vivo imaging. *Sci Rep* 6, 29490.
- [18] Poon, K.L., Brand, T., 2013. The zebrafish model system in cardiovascular research: A tiny fish with mighty prospects. *Glob Cardiol Sci Pr* 2013, 9–28.
- [19] Goessling, W., Sadler, K.C., 2015. Zebrafish: an important tool for liver disease research. *Gastroenterology* 149, 1361–1377.
- [20] Heinke, J., Patterson, C., Moser, M., 2012. Life is a pattern: vascular assembly within the embryo. *Front Biosci (Elite Ed)* 4, 2269–2288.
- [21] Tao, T., Peng, J., 2009. Liver development in zebrafish (*Danio rerio*). *J Genet Genom* 36, 325–334.
- [22] Sule, R.O., Condon, L., Gomes, A.V., 2022. A common feature of pesticides: oxidative stress—the role of oxidative stress in pesticide-induced toxicity. *Oxid Med Cell Longev* 2022, 5563759.
- [23] Mittal, M., Siddiqui, M.R., Tran, K., Reddy, S.P., Malik, A.B., 2014. Reactive oxygen species in inflammation and tissue injury. *Antioxid Redox Signal* 20, 1126–1167.
- [24] Barbalho, P.G., Lopes-Cendes, I., Maurer-Morelli, C.V., 2016. Indomethacin treatment prior to pentylenetetrazole-induced seizures downregulates the expression of il1b and cox2 and decreases seizure-like behavior in zebrafish larvae. *BMC Neurosci* 17, 12.
- [25] Brun, N.R., Koch, B.E.V., Varela, M., Peijnenburg, W.J.G.M., Spaink, H.P., Vijver, M.G., 2018. Nanoparticles induce dermal and intestinal innate immune system responses in zebrafish embryos. *Environ Sci-Nano* 5, 904–916.
- [26] Chen, X.-K., Kwan, J.S.-K., Wong, G.T.-C., Yi, Z.-N., Ma, A.C.-H., Chang, R.C.-C., 2022. Leukocyte invasion of the brain after peripheral trauma in zebrafish (*Danio rerio*). *Exp Mol Med* 54, 973–987.
- [27] Ikeda-Ohtsubo, W., Lopez Nadal, A., Zaccaria, E., Iha, M., Kitazawa, H., Kleerebezem, M., Brugman, S., 2020. Intestinal microbiota and immune modulation in zebrafish by fucoidan from Okinawa Mozuku (*Cladosiphon okamuranus*). *Front Nutr* 7, 67.
- [28] Iyer, S.S., Cheng, G., 2012. Role of interleukin 10 transcriptional regulation in inflammation and autoimmune disease. *Crit Rev Immunol* 32, 23–63.
- [29] Sullivan, G.M., Feinn, R., 2012. Using effect size—or why the P value is not enough. *J Grad Med Educ* 4, 279–282.
- [30] Brantley, S.E., Di Talia, S., 2021. Cell cycle control during early embryogenesis. *Development* 148.
- [31] Jerafi-Vider, A., Bassi, I., Moshe, N., Tevet, Y., Hen, G., Splittstoesser, D., Shin, M., Lawson, N.D., Yaniv, K., 2021. VEGFC/FLT4-induced cell-cycle arrest mediates sprouting and differentiation of venous and lymphatic endothelial cells. *Cell Rep* 35, 109255.
- [32] Takeuchi, T., 2014. Regulation of cardiomyocyte proliferation during development and regeneration. *Dev Growth Differ* 56, 402–409.
- [33] Sadler, K.C., Krahn, K.N., Gaur, N.A., Ukomadu, C., 2007. Liver growth in the embryo and during liver regeneration in zebrafish requires the cell cycle regulator, uhrf1. *Proc Natl Acad Sci USA* 104, 1570–1575.
- [34] Dutton, K., Abbas, L., Spencer, J., Brannon, C., Mowbray, C., Nikaido, M., Kelsh, R.N., Whitfield, T.T., 2009. A zebrafish model for Waardenburg syndrome type IV reveals diverse roles for Sox10 in the otic vesicle. *Dis Model Mech* 2, 68–83.
- [35] Elmaleh-Berges, M., Baumann, C., Noel-Petroff, N., Sekkal, A., Couloigner, V., Devriendt, K., Wilson, M., Marlin, S., Sebag, G., Pingault, V., 2013. Spectrum of temporal bone abnormalities in patients with Waardenburg syndrome and SOX10 mutations. *AJNR Am J Neuroradiol* 34, 1257–1263.
- [36] Andres-Delgado, L., Mercader, N., 1863. Interplay between cardiac function and heart development. *Biochim Biophys Acta* 2016, 1707–1716.
- [37] Rohr, S., Otten, C., Abdellah-Seyfried, S., 2008. Asymmetric involution of the myocardial field drives heart tube formation in zebrafish. *Circ Res* 102, e12–e19.
- [38] Chen, J.N., van Eeden, F.J., Warren, K.S., Chin, A., Nusslein-Volhard, C., Haffter, P., Fishman, M.C., 1997. Left-right pattern of cardiac BMP4 may drive asymmetry of the heart in zebrafish. *Development* 124, 4373–4382.
- [39] Liu, J., Bressan, M., Hassel, D., Huiskens, J., Staudt, D., Kikuchi, K., Poss, K.D., Mikawa, T., Stainier, D.Y., 2010. A dual role for ErbB2 signaling in cardiac trabeculation. *Development* 137, 3867–3875.
- [40] Jenni, R., Rojas, J., Oechslin, E., 1999. Isolated noncompaction of the myocardium. *N Engl J Med* 340, 966–967.
- [41] Szalai, T.E., Zhao, M., Williams, C., Oorschot, V., Parslow, A.C., Giousoh, A., Yuen, M., Hall, T.E., Costin, A., Ramm, G., Bird, P.I., Busch-Nentwich, E.M., Stemple, D.L., Currie, P.D., Cooper, S.T., Laing, N.G., Nowak, K.J., Bryson-Richardson, R.J., 2015. Zebrafish models for nemaline myopathy reveal a spectrum of nemaline bodies contributing to reduced muscle function. *Acta Neuropathol* 130, 389–406.
- [42] Chen, Z., Huang, W., Dahme, T., Rottbauer, W., Ackerman, M.J., Xu, X., 2008. Depletion of zebrafish essential and regulatory myosin light chains reduces cardiac function through distinct mechanisms. *Cardiovasc Res* 79, 97–108.
- [43] Rattka, M., Westphal, S., Gahr, B.M., Just, S., Rottbauer, W., 2021. Spen deficiency interferes with Connexin 43 expression and leads to heart failure in zebrafish. *J Mol Cell Cardiol* 155, 25–35.
- [44] Liang, D., Chang, J.R., Chin, A.J., Smith, A., Kelly, C., Weinberg, E.S., Ge, R., 2001. The role of vascular endothelial growth factor (VEGF) in vasculogenesis, angiogenesis, and hematopoiesis in zebrafish development. *Mech Dev* 108, 29–43.
- [45] Shibuya, M., 2006. Differential roles of vascular endothelial growth factor receptor-1 and receptor-2 in angiogenesis. *J Biochem Mol Biol* 39, 469–478.
- [46] Gale, N.W., Yancopoulos, G.D., 1999. Growth factors acting via endothelial cell-specific receptor tyrosine kinases: VEGFs, angiopoietins, and ephrins in vascular development. *Genes Dev* 13, 1055–1066.
- [47] Zhao, R., Watt, A.J., Li, J., Luebke-Wheeler, J., Morrissey, E.E., Duncan, S.A., 2005. GATA6 is essential for embryonic development of the liver but dispensable for early heart formation. *Mol Cell Biol* 25, 2622–2631.
- [48] Ober, E.A., Verkade, H., Field, H.A., Stainier, D.Y., 2006. Mesodermal Wnt2b signalling positively regulates liver specification. *Nature* 442, 688–691.
- [49] Goessling, W., North, T.E., Lord, A.M., Ceol, C., Lee, S., Weidinger, G., Bourque, C., Strijbosch, R., Haramus, A.P., Puder, M., Clevers, H., Moon, R.T., Zon, L.I., 2008. APC mutant zebrafish uncover a changing temporal requirement for wnt signaling in liver development. *Dev Biol* 320, 161–174.
- [50] Sosa-Pineda, B., Wigle, J.T., Oliver, G., 2000. Hepatocyte migration during liver development requires Prox1. *Nat Genet* 25, 254–255.
- [51] Huang, H., Ruan, H., Aw, M.Y., Hussain, A., Guo, L., Gao, C., Qian, F., Leung, T., Song, H., Kimelman, D., Wen, Z., Peng, J., 2008. Mypt1-mediated spatial positioning of Bmp2-producing cells is essential for liver organogenesis. *Development* 135, 3209–3218.
- [52] Noel, E.S., Casal-Sueiro, A., Busch-Nentwich, E., Verkade, H., Dong, P.D., Stemple, D.L., Ober, E.A., 2008. Organ-specific requirements for Hdac1 in liver and pancreas formation. *Dev Biol* 322, 237–250.
- [53] Farooq, M., Sulochana, K.N., Pan, X., To, J., Sheng, D., Gong, Z., Ge, R., 2008. Histone deacetylase 3 (hdac3) is specifically required for liver development in zebrafish. *Dev Biol* 317, 336–353.
- [54] Tan, X., Yuan, Y., Zeng, G., Apte, U., Thompson, M.D., Cieply, B., Stolz, D.B., Michalopoulos, G.K., Kaestner, K.H., Monga, S.P., 2008. Beta-catenin deletion in hepatoblasts disrupts hepatic morphogenesis and survival during mouse development. *Hepatology* 47, 1667–1679.
- [55] Seth, A., Ye, J., Yu, N., Guez, F., Bedford, D.C., Neale, G.A., Cordi, S., Brindle, P.K., Lemaigne, F.P., Kaestner, K.H., Sosa-Pineda, B., 2014. Prox1 ablation in hepatic progenitors causes defective hepatocyte specification and increases biliary cell commitment. *Development* 141, 538–547.
- [56] Mugoni, V., Camporeale, A., Santoro, M.M., 2014. Analysis of oxidative stress in zebrafish embryos. *J Vis Exp*.
- [57] Halliwell, B., Hoult, J.R., Blake, D.R., 1988. Oxidants, inflammation, and anti-inflammatory drugs. *FASEB J* 2, 2867–2873.
- [58] Redza-Dutordoir, M., Averill-Bates, D.A., 1863. Activation of apoptosis signalling pathways by reactive oxygen species. *Biochim Biophys Acta* 2016, 2977–2992.
- [59] Opferman, J.T., Kothari, A., 2018. Anti-apoptotic BCL-2 family members in development. *Cell Death Differ* 25, 37–45.
- [60] Luo, J., Zhang, X., He, S., Lou, Q., Zhai, G., Shi, C., Yin, Z., Zheng, F., 2020. Deletion of narfl leads to increased oxidative stress mediated abnormal angiogenesis and digestive organ defects in zebrafish. *Redox Biol* 28, 101355.